



Synthesis and evaluation of a new class of stabilized nano-chlorapatite for Pb immobilization in sediment



Jia Wan^{a,b}, Chang Zhang^{a,b}, Guangming Zeng^{a,b,*}, Danlian Huang^{a,b,*}, Liang Hu^{a,b}, Chao Huang^{a,b}, Haipeng Wu^{a,b}, Lele Wang^{a,b}

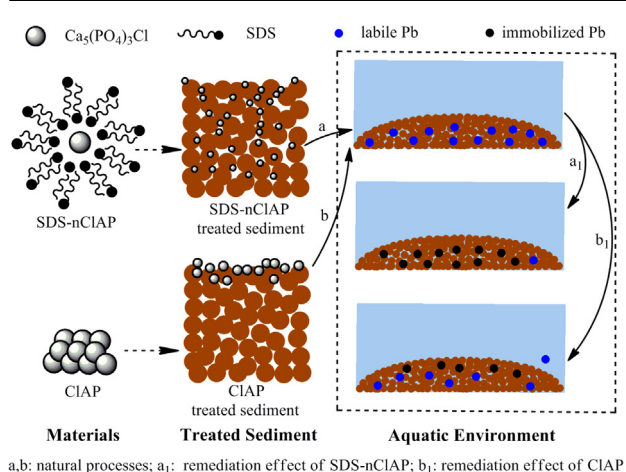
^a College of Environmental Science and Engineering, Hunan University, Changsha, Hunan 410082, China

^b Key Laboratory of Environmental Biology and Pollution Control (Hunan University), Ministry of Education, Changsha, Hunan 410082, China

HIGHLIGHTS

- SDS-nCIAP was synthesized using SDS within 40.4 nm.
- The SDS-nCIAP could effectively transform Pb labile Pb to stable fraction with a maximum increase of 38.3%.
- The SDS-nCIAP could reduce the TCLP-leachable Pb from 0.30 to 0 mg/L after 45-d treatment.
- Dissolution-precipitation process may be the main mechanism.

GRAPHICAL ABSTRACT



ARTICLE INFO

Article history:

Received 28 March 2016

Received in revised form 11 August 2016

Accepted 15 August 2016

Available online 16 August 2016

Keywords:

Sediment

Nano-chlorapatite

Pb immobilization

Leachability

Chemical speciation

ABSTRACT

During the past years, efforts have been made to deal with the Pb contaminated sediment in Xiawangang River in Hunan province, China, but it remains a serious problem since the smelting pollutants were accumulated. According to previous studies, phosphate showed an effective ability to transfer labile Pb to pyromorphite ($\text{Pb}_5(\text{PO}_4)_3\text{X}$, X=F, Cl, Br, OH) but its application was limited by its solubility and deliverability. Hence a new class of nano-chlorapatite was synthesized by using sodium dodecyl sulfate (SDS) as a stabilizer and characterized by TEM, FESEM, DLS, FTIR, and EDAX. Results demonstrated that the SDS stabilized nano-chlorapatite (SDS-nCIAP) was in spherical or spheroidal shape with a hydrodynamic diameter of 40.4 nm. Experimental data suggested that SDS-nCIAP was effective in transforming labile Pb to stable fraction with a maximum increase of 38.3%, also the reduction of TCLP-leachable Pb from 0.30 to 0 mg/L after 45-d treatment. The increase of available phosphorus in both SDS-nCIAP and CIAP treated sediment samples verified dissolution-precipitation mechanism involved in Pb immobilization. Additionally, the increment of organic matter in 10:1 treated samples was approximately 5-fold than that in 2:1 treated samples, which revealed that the micro-organisms may play an important role in it.

© 2016 Elsevier B.V. All rights reserved.

* Corresponding authors at: College of Environmental Science and Engineering, Hunan University, Changsha, Hunan 410082, China.
E-mail addresses: zgming@hnu.edu.cn (G. Zeng), huangdanlian@hnu.edu.cn (D. Huang).

1. Introduction

It is well-known that sediment plays an important role in the transportation and chemical-speciation-transformation of heavy metals since it is the largest container and sources of metals in the aquatic ecosystem [1,2]. The sediment from lakes, harbors or rivers which located in the industrial areas, especially the metal smelter, received the most of industrial wastewater containing lots of heavy metals, leading to seriously heavy metal pollution in sediment [3]. Once the heavy metals are exposed to the organisms, the detrimental effects to the plants, microbes, animals and humans should not be neglected [4–12]. Thus it is necessary to find an effective method to remedy the polluted sediment [13–15]. Accordingly, the main factor we need to take into consideration is the chemical speciation of heavy metals which greatly associates with the transportation and mobilization of the heavy metals in sediment [16] while the total content of heavy metals in sediment could not give any effective information about the physical and chemical behaviors of the heavy metals in most cases [3]. BCR (European Community Bureau of Reference) sequential extraction method divides the heavy metal into four speciations: acid soluble/exchangeable fraction (F1) and reducible fraction (F2), both of which can be easily leached into environment and result in a direct damage to the organisms [2]; oxidizable fraction (F3), which can be transformed into F1 and F2 with the change of redox potential and pH, showing a potential eco-toxicity to the organisms [17]; the last is the residual fraction (F4) which is universally accepted as the most stable fraction and almost unreactive under a wide range of natural conditions [1,18].

Different approaches used in dealing with contaminated sediments can be divided into *ex situ* and *in situ* methods in general which mostly depend on the characteristics of sediments [19]. Phosphate amendments have been widely recognized as a low-cost, effective and non-disruptive *in situ* remediation method for heavy metal polluted solid wastes. And the phosphate has a perfect immobilized efficiency in Cu(II), Zn(II), and Cd(II), especially the Pb(II), which can be transferred to the most strongly bound Pb fraction presented as pyromorphite ($\text{Pb}_5(\text{PO}_4)_3\text{X}$, X=F, Cl, Br, OH) with the remediation of phosphates [20–23]. In previous studies, particulate phosphate and soluble phosphate salts were commonly used in metal immobilization [24]. The soluble phosphate salts can dissolve easily in sediment-solution with a high mobility and they could supply more effective phosphorus (P) for metal immobilization [25], but it may greatly increase the environmental risk of eutrophication by releasing excessive P. On the other hand, even the fine-ground particulate phosphates are hardly delivered to the contaminated zone in sediment due to its large size and lower solubility, which is unfavourable for the *in situ* remediation [22]. Thus it is urgent to investigate a new class of phosphate for the sediment remediation.

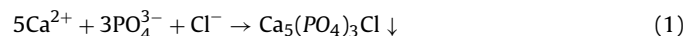
Based on the previous studies of Liu and Zhao [24,26,27], a new class of nano-chlorapatite was synthesized in this study by using sodium dodecyl sulfate (SDS, an anionic surfactant with the formula $\text{CH}_3(\text{CH}_2)_{11}\text{OSO}_3\text{Na}$) as a stabilizer and characterized by dynamic light scattering (DLS), transmission electron microscopy (TEM), field emission scanning electron microscope (FESEM), fourier transform infrared spectrometry (FTIR) and energy dispersive X-ray (EDAX). In order to investigate the Pb immobilization effect of the synthesized nano-chlorapatite on the polluted sediment, the leachable Pb fraction and the chemical speciation of Pb were detected in the experiment. Moreover, the available phosphates and organic matter were also observed in this research for analyzing the possible interaction mechanisms between the nano-particles and the sediment [28–30].

2. Materials and methods

All the chemicals used in this experiment were of analytical or higher grade. All the containers and equipments were washed extensively with ultrapure water from an Ultra-pure Water System and all the solutions were prepared with the ultrapure water. The experiment was conducted in triplicate and the results were expressed as mean \pm standard deviation.

2.1. Synthesis and characterization of SDS-nClAP

SDS stabilized chlorapatite nanoparticles (SDS-nClAP) was synthesized in this study by following the steps below: Firstly, dissolved the SDS, $\text{CaCl}_2 \cdot 2\text{H}_2\text{O}$ and $\text{Na}_3\text{PO}_4 \cdot 12\text{H}_2\text{O}$ into the ultrapure water to achieve the solutions of 1% (w/w) SDS, 26.8 mM Ca^{2+} and 16 mM PO_4^{3-} , respectively. Then under the constantly mixing (magnetic stirrer with a Teflon-coated stir bar) at 1000 r/min, 12.5 mL of 26.8 mM Ca^{2+} were added into 25 mL 1% (w/w) SDS solution using an acid burette at a steady speed of 5~8 drops per minute. After stirring for 12 h, another 12.5 mL of 16.0 mM PO_4^{3-} were added into the mixture dropwise by the acid burette (5~8 drops per minute) with constantly mixing at 1500 r/min. To give a visually comparison between the chlorapatite particles (ClAP) and SDS-nClAP, a ClAP suspension start with 25 mL ultrapure water instead of 25 mL 1% (w/w) SDS solution was prepared with other conditions unchanged. For the completely formation of the SDS-nClAP, the mixture was continued stirred for 12 h at 1500 r/min after the titration reached the end. Then an amount of 50 mM HCl were used to make the final pH of the two suspensions to 6.0. The details were summarized in laboratory flowchart shown in Fig. 1. The molar ratio of Ca^{2+} to PO_4^{3-} was chosen according to the chemical formula of ClAP represented as $\text{Ca}_5(\text{PO}_4)_3\text{Cl}$, which generated through the following equation [24]:



The hydrodynamic diameters of synthesized SDS-nClAP were characterized by DLS. The TEM samples were prepared by placing a drop of the SDS-nClAP suspension on a carbon-coated copper grid and dried at 28 °C for 24 h, then the TEM images were taken by a JEM-3010 (JEOL, Japan) at 120 kV to observe the cross section structure of the material. For analyzing the surface morphology, the freeze-dried material was placed on a piece of double coated carbon conductive tape and sprayed by gold for several seconds, then FESEM was conducted by a JSM-6700 (JEOL, Japan) along with an EDAX attachment. The functional groups on the surface of SDS-nClAP were analyzed by the KBr pellet method using a Shimadzu FTIR spectrophotometer (IRAffinity-1) at spectral range varying from 4000 to 400 cm^{-1} .

2.2. Sample collection and preparation

The sediment samples were collected from Xiawangang River in Zhuzhou, Hunan province in China. All the sediment samples were tiled on a cardboard, dry naturally for 5~7 d and then sieved through a 2 mm nylon sieve to remove the coarse debris. After this, the dried sediment was placed in a mortar, ground by a pestle then sieved to <150 μm . All the samples were stored at 4 °C and keep dry before being used. Some properties of the sediment and the concentrations of heavy metals in sediment samples along with the national standard of heavy metals in China are listed in Table 1. The Pb concentration in sediment samples ($589.7 \pm 13.2 \text{ mg/kg}$) was more than 1.5 times of the national standard (350 mg/kg), showing a big threat to the organisms.

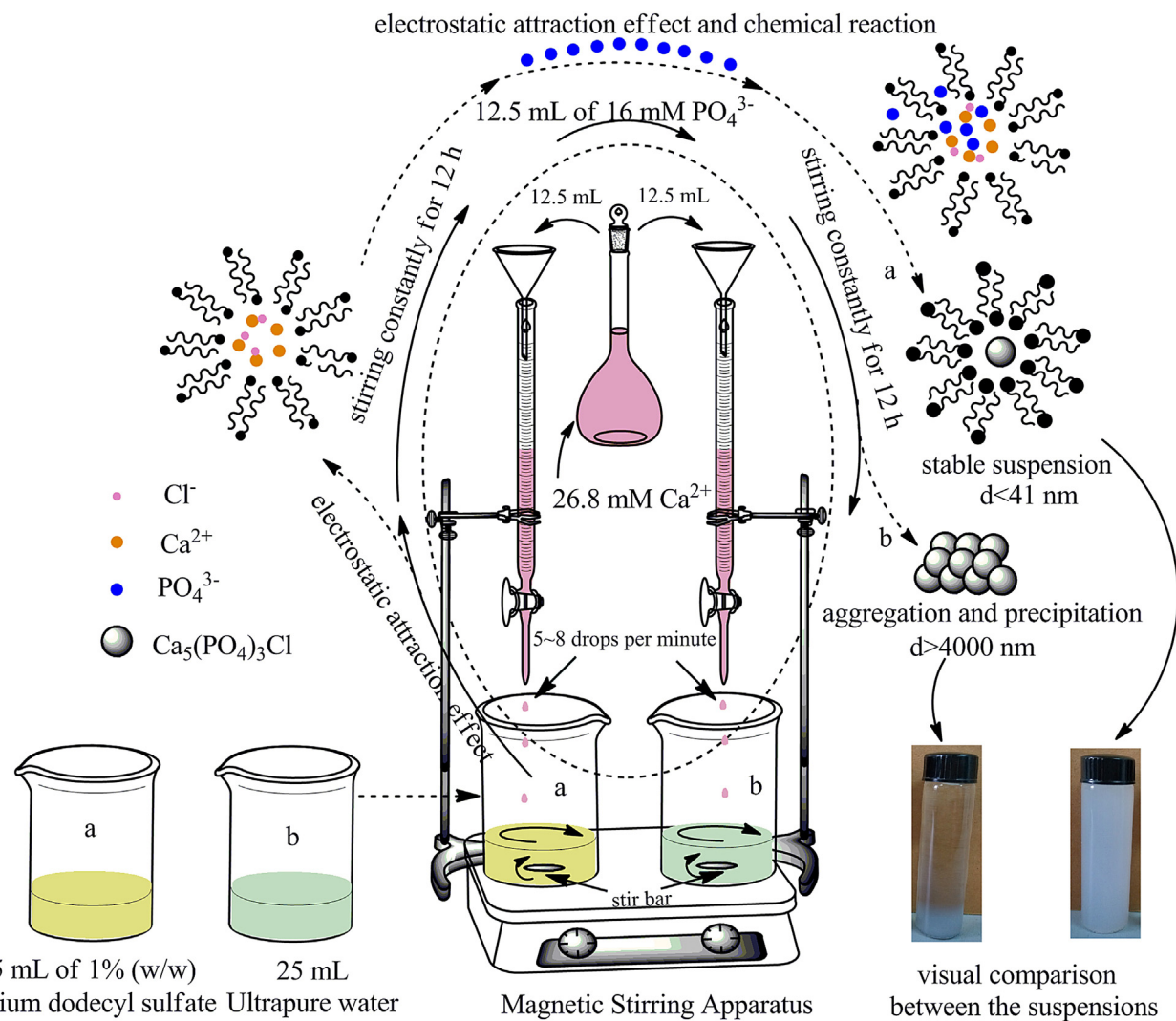


Fig. 1. Laboratory flowchart of the experiment.

Table 1

Some properties and heavy metal concentrations in sediment samples and the national application standards of heavy metals in sediment. (mean \pm standard deviation, $n \geq 3$).

Metals/Properties	(mg/kg)/(%)	National Application Standard (mg/kg)		
		pH > 7.5	pH 6.5 ~ 7.5	pH < 6.5
Pb	589.7 \pm 13.2	350	300	250
Cu	200.8 \pm 6.9	100	100	50
Fe	47100 \pm 213	–	–	–
pH	7.98 \pm 0.02	–	–	–
Moisture content (dried sediment)	0.783 \pm 0.11%	–	–	–
Total organic matters	5.9 \pm 0.12%	–	–	–

2.3. Sediment remediation experiment

For sediment remediation, 0.5 g (2.5 g, for the measurement of available phosphorus) stored sediment were placed in a 15 mL (50 mL) circled plastic centrifuge tube, then 1 mL (5 mL) SDS-nCIAP suspension were added into the centrifuge tube to achieve a suspension-to-sediment ratio of 2:1 (mL/g). To analyze the relationship between the immobilization efficiency and the addition amount of the SDS-nCIAP, 5 mL (25 mL) of the SDS-nCIAP suspension were added into the centrifuge tube which contains 0.5 g (2.5 g) stored sediment to form a suspension-to-sediment ratio of 10:1 (mL/g). Then all the samples were shaken for a few minutes for completely mixed. The control experiment was conducted with

CIAP suspension instead of SDS-nCIAP suspension with other conditions unchanged. The samples were treated for 1 ~ 45 days then centrifuged at 4000 r/min for 20 min, the supernatant and sediment were separated and stored respectively for the further measurement.

2.4. BCR experiment

50 mL centrifuge tube which contains 0.5 g treated sediment was used for the measurement of the heavy metal speciation. The BCR sequential extraction procedure according to Rauret et al. [31,32] was conducted with some modifications following the steps in Table 2.

Table 2

The BCR extraction method used in this study.

Speciations	Methods
Acid soluble fraction (F1)	(1) 40 mL 0.11 mol/L CH ₃ COOH (2) shaken at 250 r/m for 16 h (3) centrifuged at 4000 r/m for 20 min
Reducible fraction (F2)	(1) 40 mL 0.5 mol/L NH ₂ OH·HCl (freshly prepared, pH = 2.0, using 0.5 mol/L HNO ₃) (2) shaken at 250 r/m for 16 h (3) centrifuged at 4000 r/m for 20 min
Oxidizable fraction (F3)	(1) 10 mL H ₂ O ₂ , kept at 85 °C until the mixture volume was less than 3 mL (2) 10 mL H ₂ O ₂ , kept at 85 °C until the mixture volume was less than 1 mL (3) 50 mL NH ₄ OAc (pH = 2.0, using HNO ₃) (4) shaken at 250 r/m for 16 h (5) centrifuged at 4000 r/m for 20 min
Residual fraction (F4)	(1) a mixture of 5 mL HNO ₃ , 5 mL HF and 3 mL HClO ₄ (2) 90 °C for 40 min, 140 °C for 60 min, 170 °C for 40 min (3) dilute the products with ultrapure water to a volume of 100 mL

The liquid extract after filtration through a 0.45 μm glass fiber filter was stored at 4 °C before being measured by flame atomic absorption spectrometry (AAS700, PerkinElmer, USA). The results were checked by comparing the sum of all fractions with the total heavy metal concentration [3,16]. The recovery rates of Pb in this experiment were ranging from 93% to 108% and it was in good agreement with other researchers [16,33], ensuring the precision and reliable of the data.

2.5. Toxicity characteristic leaching procedure (TCLP)

The toxicity characteristic leaching procedure (TCLP) was conducted according to the method described by Xenidis et al. [34,24]. The extraction fluid was prepared by diluting 5.7 mL CH₃COOH with ultrapure water to a volume of 1000 mL, using 1 mol/L HNO₃ to achieve pH = 2.88 ± 0.05. Mixed 10 mL extraction fluid with 0.5 g sediment in a 15 mL centrifuge tube and shook it (32 r/min) for 19 h at 25 °C. Then centrifuged the tube at 4000 r/min for 20 min, the supernatant after filtration through a 0.45 μm glass fiber filter was defined as the TCLP extract. Adjusted the pH of the TCLP extract to 2.0 by HNO₃ and stored at 4 °C before being analyzed by AAS.

2.6. Available phosphorus (AP) and organic matter (OM)

In order to determine the AP level in the sediment, the molybdenum-antimony anti-spectrophotometric method previously described [35,36] was used and the standard curve was prepared from known concentration of KH₂PO₄ (from 0 ~ 0.5 μg·mL⁻¹). To determine the OM of the sample, the dilution heating method described by Nelson et al. [37] was used and the OM was calculated by the equation presented as follows:

$$OM = \left[\frac{0.5 \times (V_0 - V) \times 0.001 \times 3.0 \times 1.33}{W_0 K_2} \right] \times 1000 \times 1.724 \quad (2)$$

Where V₀ is the FeSO₄ consumption of the blank, the V is the FeSO₄ consumption of the sample, W₀ is the weight of the sediment and K₂ represent the moisture content of the sample.

3. Results and discussions

3.1. Characterization of SDS-nCIAP

The morphology of the SDS-nCIAP was characterized by FESEM and TEM. Fig. 2A is the TEM image of synthesized SDS-nCIAP. From

the TEM image we can see that the average diameter of these particles was estimated at approximately 10 nm. To further reveal the morphology of the nanoparticles, a FESEM microphotograph was presented in Fig. 2B. From Fig. 2B we can see the nanoparticles are in a spherical or spheroidal shape with a diameter ranging from a few nm to 100 nm. The DLS analysis, which has been employed to measure the particle diameter in this experiment [38], showed that the mean hydrodynamic diameters of SDS-nCIAP and CIAP in suspensions were 40.4 nm and 4100 nm, respectively. It has been reported by He and Zhao that the CMC macromolecules which are invisible under TEM could result in an overestimated particle size with DLS [39]. Therefore, in this experiment the SDS macromolecules may be responsible for the discrepant results between DLS and TEM [39]. On the other hand, the freeze-dried nanoparticles' powder was the gather of the particles thus the particle diameter was more nonuniform than DLS and TEM [40]. Fig. 2C is the EDAX spectrum of the gray spherical substance in FESEM image. There were some obvious peaks of C, O, Na, P, S, Cl and Ca in the EDAX spectrum, demonstrating that the gray spherical substance in FESEM image contained all the elements existed in SDS-nCIAP except H which cannot be detected by EDAX.

The interaction between the chlorapatite and SDS during the preparation of SDS-nCIAP was confirmed by the FTIR spectra. The IR spectra (b) showed in Fig. 2D demonstrated the characteristic peaks of pristine SDS while these absorption bands were also observed in the spectrum of the SDS-nCIAP (Fig. 2D (a)), indicating that there were no significant changes in the surface properties and the functional groups of SDS before and after the formation of SDS-nCIAP. These results revealed that the SDS cooperated with chlorapatite particles by an electrostatic effect or other physical forms instead of chemical reaction, ensuring a stable property of the chemicals.

3.2. Effects of nanoparticle treatment on Pb immobilization in sediment

3.2.1. Chemical speciation of Pb

The chemical speciation distribution of Pb estimated by BCR procedure in SDS-nCIAP treated and CIAP treated sediment were shown in Fig. 3a and Fig. 3b, respectively. Pb was mainly bound to F3 (approximate 60.5%) in the original sediment while the F1, F2 and F4 occupied 8.2%, 11.1% and 20.2%, respectively. From Fig. 3 we can see that Pb distribution in various fractions showed a similar change during the treated period whether amended by SDS-nCIAP or CIAP: F4 was time-dependent increased while the F1 and F2 were time-dependent decreased, on the other hand, F3 exhibited no obvious change with the treated time as compared to other three fractions. This phenomenon may result from the immobilization effect of PO₄³⁻ contained in the two kinds of materials, which has been proved to be an excellent amendment for *in situ* remediation of Pb polluted sediment [24]. Once the labile Pb reached the phosphate materials, the Pb could be immobilized into a mineral structure substance which was expressed as chlor-pyromorphite with a low K_{sp} (10^{-84.4}), and it was in accordance with Liu and Zhao's study [24]. A more sizable increase of F4 in sediment was observed in SDS-nCIAP treated samples after 45-d treatment than CIAP treated samples when treated at the same ratio, indicating that SDS-nCIAP had a better effect on Pb immobilization. It has been known that solid phosphates are hardly delivered to the contaminated zone in sediment, which limits the reaction of phosphates with heavy metals. From the visual comparison between SDS-nCIAP and CIAP (Fig. 1) we can see that SDS-nCIAP exhibited a more stable characteristic than the CIAP since the former could maintain for nearly a month without obvious precipitation while the later may precipitate in a few hours. Additionally, the DLS results also showed that the CIAP particles were much bigger than SDS-nCIAP particles, which was unfavourable for the Pb immobilization. Thus

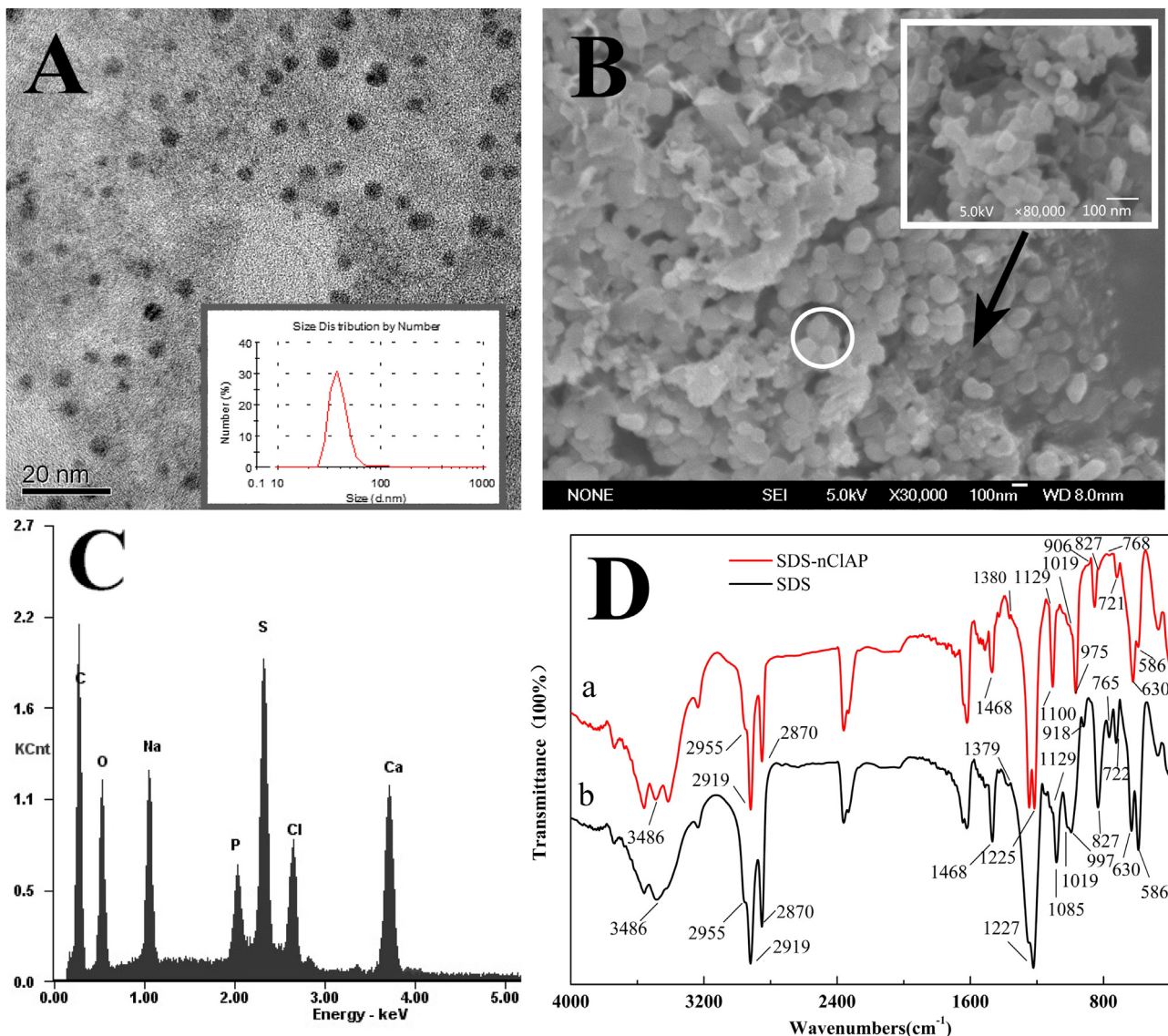


Fig. 2. Characterization of the synthesized SDS-nCIAP: (A) TEM image. The hydrodynamic diameters of synthesized SDS-nCIAP were shown at the right corner. (B) FESEM image. (C) EDAX analysis of the gray spherical substance in the white circle on FESEM image. (D) FTIR spectra of SDS-nCIAP (a) and pure SDS (b) in the region between 400 and 4000 cm^{-1} , respectively.

the nano-sized SDS-nCIAP may be more easily to react with Pb, showing higher immobilization efficiency. Simultaneously, owing to the high level of PO_4^{3-} provided by the materials, the high-ratio treated samples were more efficient in Pb immobilization.

F1 and F2, which two were considered to be the most weakly bound fraction of Pb and had direct toxicity to the organisms [2], showed a time-dependent decrease in both Fig. 3a and Fig. 3b. Additionally, from the comparison between Fig. 3a and Fig. 3b we can see that the SDS-nCIAP treated samples performed better than CIAP treated samples. Pb in F1 can be easily released to the environment and converted into free ions, and then the Pb was readily to react with PO_4^{3-} and subsequently formed Pb-phosphate, inducing the reduction of F1 and the increasement of F4. Although F2 of Pb was stable than F1, the external conditions changes such as pH or the anoxic conditions induced by the addition of SDS-nCIAP and CIAP ($\text{pH}=6$) may also lead the release of F2, then it was immobilized by phosphate materials [41,42]. At the same time, it can be easily found that the SDS-nCIAP was more effective to immobilize F1 and F2 than the CIAP when treated with the equal amount of these two materials for 45 d. As a result of 45-d treatment, the F3 of

Pb was slightly decreased by about 6% in all the samples except the SDS-nCIAP treated sample at ratio of 10:1, which experienced a sharp decline about 20%. It seems that the F3 was more difficult to be transformed into F4 than F1 and F2 since F3 was usually complexed or peptised by the natural organic substances and it was relatively stable, but when the organic matter was attacked by oxidative effect, the soluble metals would be liberated and available for organisms [42]. Generally speaking, the organically bound Pb (F3) could be transferred to pyromorphite (F4) with the present of phosphate since the later was more thermodynamically stable ($K_{\text{sp}}=10^{-84.4}$). As been mentioned above, the SDS-nCIAP could be more easily to be delivered and react with Pb owing to its nano-size, which was favorable for the transformation of F3 as well. On the other hand, the high level of smaller nanoparticles may disrupt the electron transport loci on bacterial membrane and cause oxidation effect, which may promote the release of F3 [43]. Therefore, in case of SDS-nCIAP treated sample at ratio of 10:1, about 20% of Pb in F3 was transformed into F4, which was much higher than other samples.

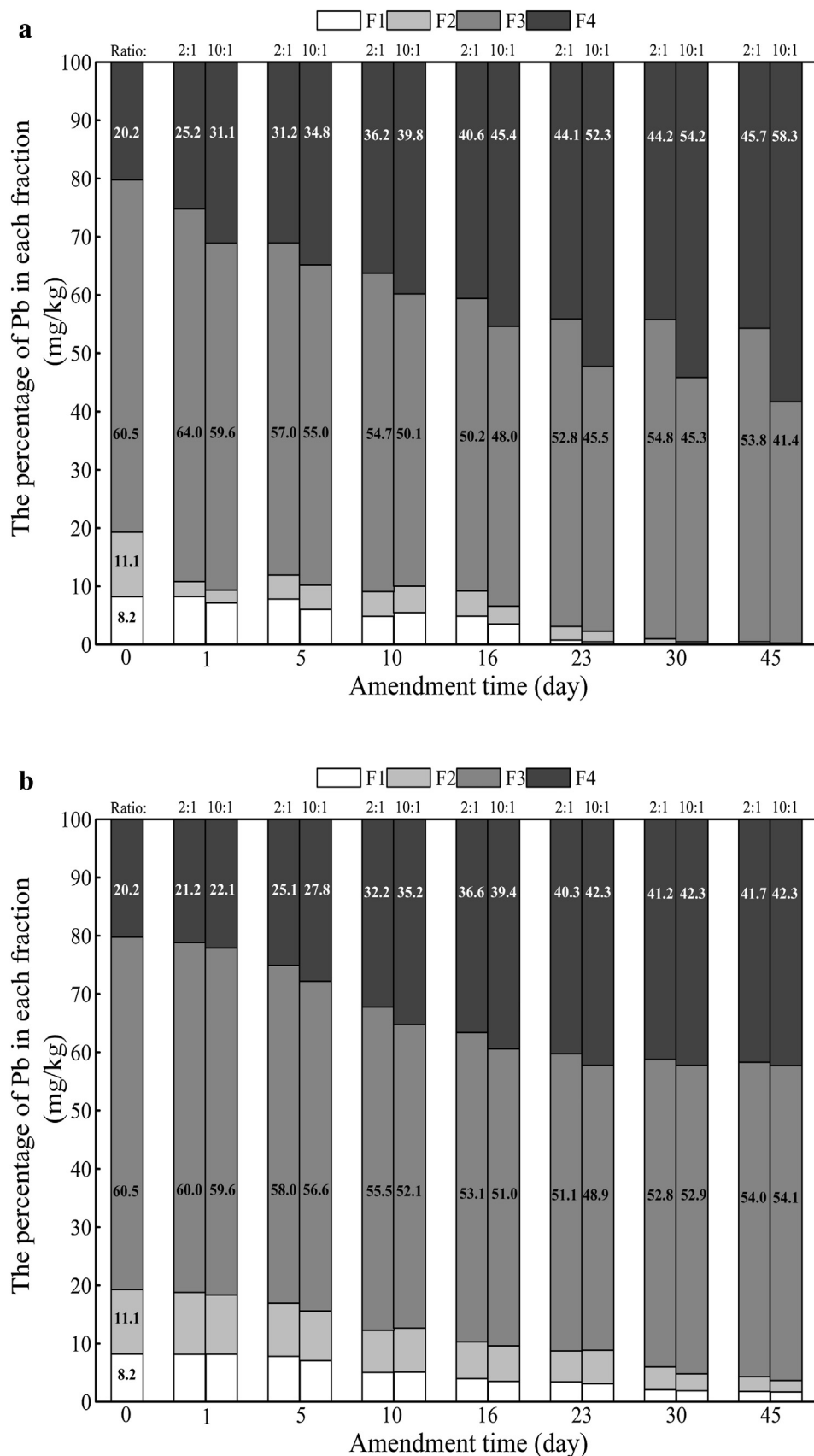


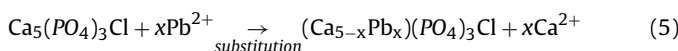
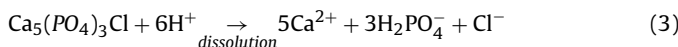
Fig. 3. The percentage of each chemical speciation (F1, F2, F3 and F4) of Pb in SDS-nClAP (a) and ClAP (b) amended sediment during 45-d treatment at ratio of 2:1 and 10:1, respectively. Day 0 represents the level of untreated sediment.

3.2.2. TCLP leachability of Pb

The TCLP was recognized as the standard method to assess the leaching toxicity of Pb in sediment and it was improved on the basis of hazardous waste extraction procedure (EP) by USEPA [44]. The change of TCLP-leachable Pb and its reduction efficiency in the SDS-nCIAP and CIAP treated sediment were shown in Fig. 4a and Fig. 4b, respectively.

In Fig. 4 we can find that the original TCLP-leachable Pb of the sediment was 0.30 mg/L, which was lower than USEPA's limit (5 mg/L) but still have potential threat to the organisms. Pronounced reductions of the TCLP leachable Pb content were found in both SDS-nCIAP and CIAP treated samples during 45-d amendment (Fig. 4), especially in the SDS-nCIAP treated sediment which the mean Pb leachable concentration was sharply reduced from 0.30 to 0 mg/L with 100% treatment efficiency after 45-d treatment. It should be noticed that the amount dependent effect appeared in Fig. 3 was also occurred in the reduction of TCLP-leachable Pb (Fig. 4). Fig. 4a showed that it took 30 d for 10:1 treated samples to reach 100% reduction efficiency of TCLP-leachable Pb while it need 45 d for 2:1 treated samples to achieve the same effect. The similar trend could also be found in Fig. 4b although the sediment amended by CIAP exhibited lower reduction efficiency. Attributed to the better Pb-immobilization ability of SDS-nCIAP (Section 3.2.1), it showed a higher reduction efficiency of TCLP-leachable Pb than the CIAP through transferring the F1, F2 and F3 fraction of Pb to F4 fraction effectively, which directly reduced the Pb toxicity and leachability.

The explanation for the reduction of TCLP-leachable Pb may attribute to the theory that the labile fraction of Pb could be transformed into strongly bound Pb-phosphate fraction (pyromorphite) with the amendment of phosphate materials. A number of researches have detected direct evidence for pyromorphite formation in phosphate amended soils [45–50]. Based on the studies of former researchers, the mechanism shown in the below equations was the main explanation for the decrease of TCLP-leachable Pb and the increase of F4 mentioned in Section 3.2.1 [24,50–53]:



Eqs. (3) and (4) reveal the immobilization process through the dissolution of $\text{Ca}_5(\text{PO}_4)_3\text{Cl}$ and subsequently the precipitation of $\text{Pb}_5(\text{PO}_4)_3\text{Cl}$, which has been considered as the main mechanism for Pb immobilization in sediment. Another mechanism for the $\text{Pb}_5(\text{PO}_4)_3\text{Cl}$ formation proposed by Suzuki et al. and Takeuchi et al. [51,52,54] was the substitution (ion exchange) effect, as shown in Eq. (5), the Pb(II) is substituted for Ca(II) in the chlorapatite structure, then the $\text{Pb}_5(\text{PO}_4)_3\text{Cl}$ was formed. These two mechanisms could be the main reason that responsible for the change of TCLP-leachable Pb and chemical speciation of Pb.

3.2.3. Potential mechanism and environmental risk of nanoparticle treatment

The results we mentioned above (3.2.1 and 3.2.2) revealed that the main factors influenced the immobilization efficiency of Pb in the sediment were: 1) the species of the stabilization materials: the SDS-nCIAP had more advantages in immobilizing Pb and reducing the TCLP-leachable Pb content than CIAP; 2) the addition amount of the materials: the 10:1 treated samples always showed a high stabilization efficiency of Pb than 2:1 treated samples. According to Thawornchaisit's study [55], the stabilization efficiency of phosphates has a positive correlation with its solubility since the easy dissolved phosphates could release more effective groups such

as PO_4^{3-} to immobilize Pb in the sediment. Since the AP will be released through the dissolution of $\text{Ca}_5(\text{PO}_4)_3\text{Cl}$ (Eq. (3)) and consumed by the precipitation of $\text{Pb}_5(\text{PO}_4)_3\text{Cl}$ (Eq. (4)), the AP may have a direct relationship with the Pb immobilization process in treated sediment.

Fig. 5 exhibited the AP levels of treated samples during the amendment process. From Fig. 5 we can observe that the AP levels were increased after the addition of SDS-nCIAP and CIAP, indicating the dissolution mechanism of $\text{Ca}_5(\text{PO}_4)_3\text{Cl}$ (Equation 3). After 15-d amendment, the AP experienced a decrease and at the same time F4 was increased (Fig. 3), which may attribute to the formation of Pb-phosphate (Eq. (4)). The treated samples with 10:1 ratio always had higher AP levels than the samples treated with 2:1 ratio whether in SDS-nCIAP or CIAP amended samples (Fig. 5), providing a favorable condition for Pb stabilization (concluded from Fig. 3 and Fig. 4). As a consequence of the shortage of AP, the samples treated with lower ratio could not supply enough PO_4^{3-} for Pb immobilization in sediment, resulting in an amount-dependent effect (showed in Figs. 3 and 4). However, it can be seen from Fig. 5 that the AP levels in CIAP treated samples appeared to be always higher than SDS-nCIAP treated samples when amended at the same ratio, which seems to be benefit for the Pb immobilization. But actually, we have confirmed from Fig. 3 and 4 that the SDS-nCIAP performed more effective in immobilizing Pb in the sediment than CIAP. The reasonable explanation for this result should be that the SDS-nCIAP can be delivered more easily to the contaminated sediment to supply PO_4^{3-} for the Pb immobilization than CIAP owing to its nano-size and stable composition. These characteristics make the SDS-nCIAP more effective for Pb immobilization and accelerate the depletion of AP. Additionally, the PO_4^{3-} provided by CIAP would be limited by its mobility and retained on the upper part of the sediment with the gather of CIAP, then failed to immobilize Pb in deep part, resulting in a high level of AP remained.

On the other hand, the excessive AP generated during the amendment could induce a potential effect on eutrophication of groundwater and surface water [22,56,57], becoming an intractable problem. Thus the SDS-nCIAP may be a desirable remediation material since it could immobilize Pb more efficiently than CIAP by enhancing the effectiveness of PO_4^{3-} . Consequently, the SDS-nCIAP showed more advantages than CIAP during the amendment of the sediment, suggesting that the material delivering ability and effective utilization of P may be the main factors that need to be taken into consideration for the phosphate applications.

3.3. Exploration of the inner-mechanism: change of OM

OM has been identified as one of the most important sediment components since it is involved in the binding of metals to sediment [58,59]. Thus the variation of OM in treated samples were detected and summarized in Fig. 6. As shown in Fig. 6, the D-values between these two kinds of treated sediment were ranging from 0.07 to 2.95 g/kg at ratio 2:1, 0.01–3.51 g/kg at ratio 10:1, respectively, which were almost no differences between the equal-ratio treated samples. Moreover, an interesting finding appeared in the course of treatment that the OM increment in 10:1 treated samples was approximately 5-fold than that in 2:1 treated samples, showing a positive correlation with the addition amount of the materials. It has been reported that the enzymatic activities and biomass of micro-organisms in sediment were related to the contamination of heavy metals and low molecular weight organic acids secreted by the organisms can increase stable metal-phosphate complexes in response [60,61]. On the other hand, the original sediments were natural dried before used, which is not suitable for micro-organism growth, thus the addition of SDS-nCIAP and CIAP suspensions may improve the survival environment of micro-

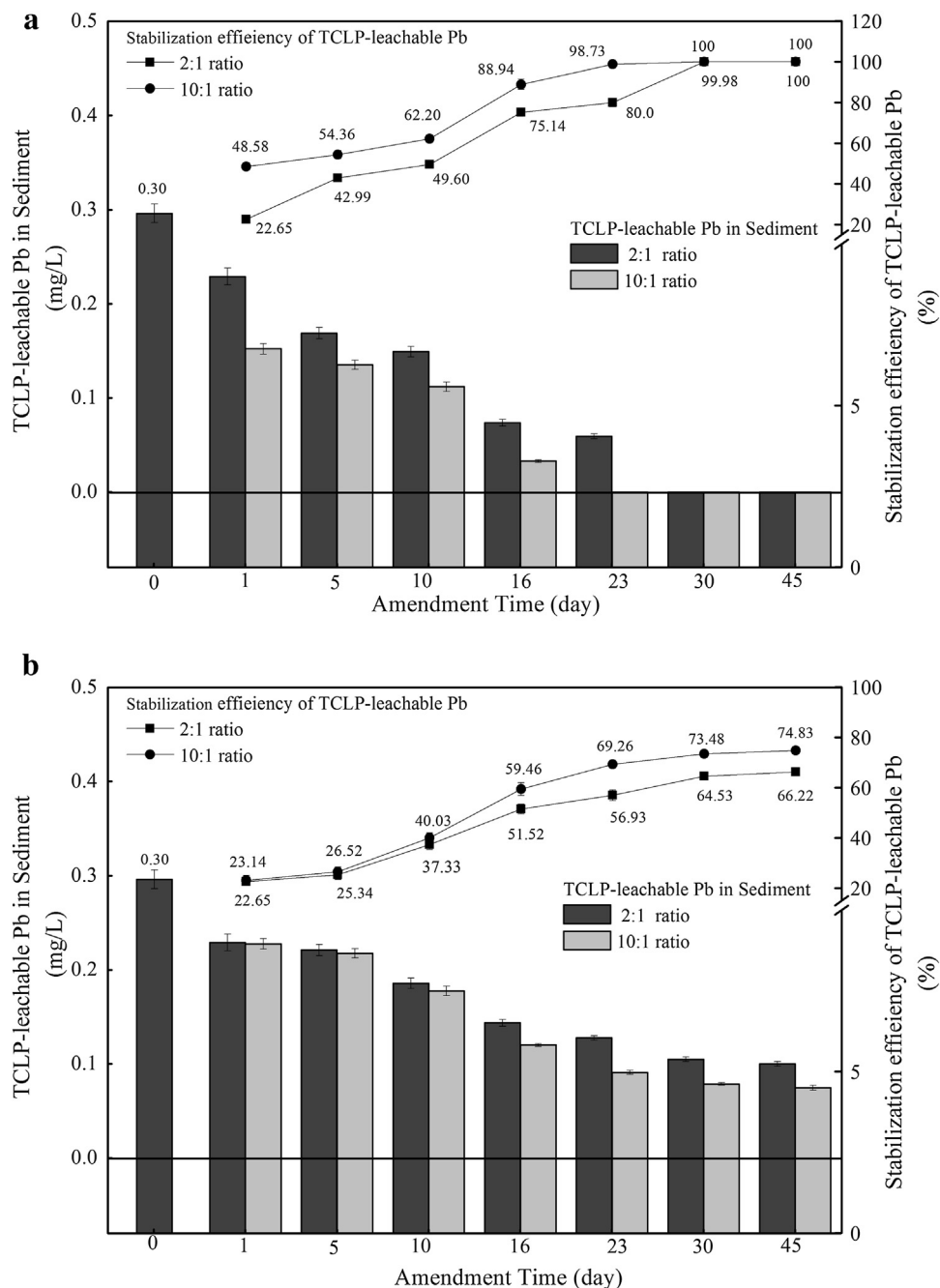


Fig. 4. The TCLP-leachable Pb fraction in SDS-nCIAP (a) and CIAP (b) amended sediment during 45-d treatment at ratio of 2:1 and 10:1, respectively. The error bars represent the standard deviation of the means ($n=3$) and day 0 represents the level of untreated sediment.

organism by neutralizing the Pb toxicity and supplying SDS , Ca^{2+} , PO_4^{3-} and H_2O . Consequently, the SDS-nCIAP and CIAP suspensions may induce an amount-dependent increase in OM content by promoting the micro-organisms to secrete organic compound. According to the study of Lin and Chen [62], the OM is the important scavenger for metals in sediments. They have also demonstrated that the adsorbability of heavy metal of the sediment was increased with the increasing of OM contents, which was consistent with our findings in Section 3.2. That is to say the behavior of micro-organisms may also be an important mechanism involved in the Pb immobilization in the sediment and it was worth studying in the further.

4. Conclusions

In this study, a new class of nano-chlorapatite was synthesized using SDS as a stabilizer for Pb immobilization in contaminated sediment in Xiawangang River. The product nano-chlorapatite was characterized by TEM, FESEM, DLS, FTIR, and EDAX, and these results showed that the chlorapatite particles were existed as stable nanoparticles within 40.4 nm in the SDS solutions. Laboratory tests showed that both the SDS-nCIAP and CIAP could transfer the Pb from unstable fraction to stable fraction and at the same time decrease the TCLP-leachable Pb fraction in sediment after 45 days of treatment. Owing to its nano-size and stable composition, the synthesized SDS-nCIAP not only performed more effectively in Pb immobilization than CIAP, showing a time- and amount-dependent

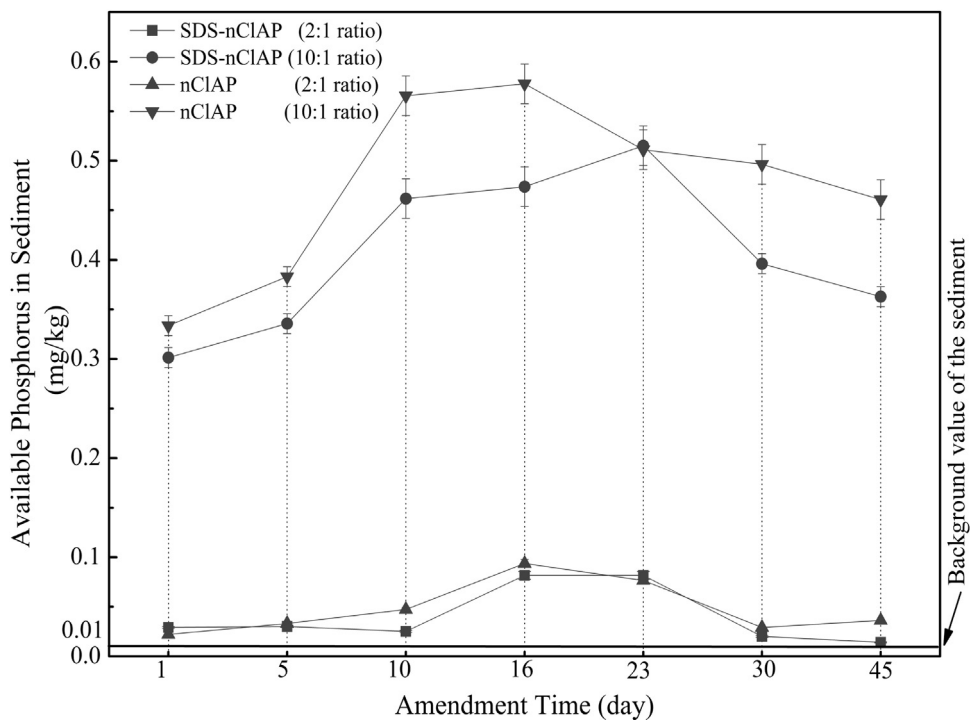


Fig. 5. Available phosphorus in the SDS-nCIAP amended samples and CIAP amended samples at ratio of 2:1 and 10:1 during 45-d treatment, respectively. The error bars represent the standard deviation of the means ($n=3$) and the line of the background value represents the level of untreated sediment.

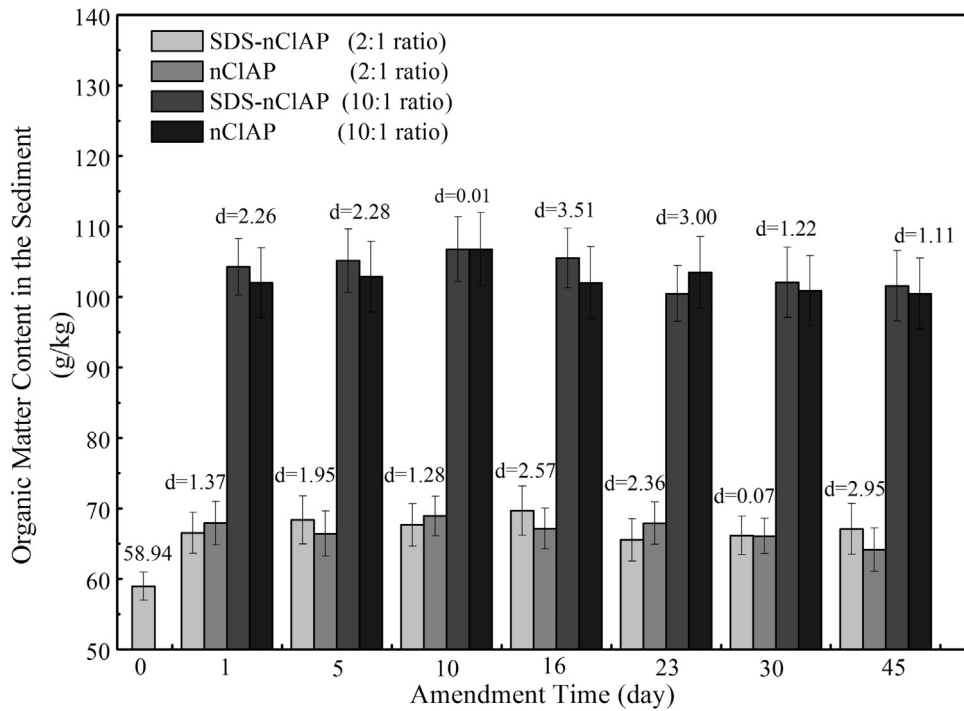


Fig. 6. The change of organic matter in amended sediment during 45-d treatment. The error bars represent the standard deviation of the means ($n=3$) and day 0 represents the level of untreated sediment.

effect simultaneously, but could also introduce less AP into the sediment when compared with CIAP, reducing the eutrophication risk induced by the phosphate material. The increase of AP in both SDS-nCIAP and CIAP treated sediment samples verified the dissolution-precipitation mechanism involved in Pb immobilization. Additionally, the increment of organic matter in 10:1 treated samples was approximately 5-fold than that in 2:1 treated samples,

which revealed that the micro-organisms may play an important role in it. However, the optimum addition amount of the SDS-nCIAP and how does the micro-organisms influence the Pb immobilization in contaminated sediment are still unknown and need to be investigated in further studies.

Acknowledgements

This study was financially supported by the National Natural Science Foundation of China (51521006, 51378190, 51278176, 51579098 and 51108178), the Environmental Protection Technology Research Program of Hunan (2007185), the Program for New Century Excellent Talents in University (NCET-13-0186), Scientific Research Fund of Hunan Provincial Education Department (521293050) and the Program for Changjiang Scholars and Innovative Research Team in University (IRT-13R17).

References

- [1] C. Zhang, Z.G. Yu, G.M. Zeng, M. Jiang, Z.Z. Yang, F. Cui, M.Y. Zhu, L.Q. Shen, L. Hu, Effects of sediment geochemical properties on heavy metal bioavailability, *Environ. Int.* 73 (2014) 270–281.
- [2] M. Jiang, G. Zeng, C. Zhang, X. Ma, M. Chen, J. Zhang, L. Lu, Q. Yu, L. Hu, L. Liu, Assessment of heavy metal contamination in the surrounding soils and surface sediments in Xiawanggang River, Qingshuitang District, *PLoS One* 8 (2013).
- [3] L. Wang, X. Yuan, H. Zhong, H. Wang, Z. Wu, X. Chen, G. Zeng, Release behavior of heavy metals during treatment of dredged sediment by microwave-assisted hydrogen peroxide oxidation, *Chem. Eng. J.* 258 (2014) 334–340.
- [4] C. Zhang, N. Song, G.M. Zeng, M. Jiang, J.C. Zhang, X.J. Hu, A.W. Chen, J.M. Zhen, Bioaccumulation of zinc lead, copper, and cadmium from contaminated sediments by native plant species and *Acrida cinerea* in South China, *Environ. Monit. Assess.* 186 (2014) 1735–1745.
- [5] C. Zhang, C. Lai, G.M. Zeng, D.L. Huang, C.P. Yang, Y. Wang, Y.Y. Zhou, M. Cheng, Efficacy of carbonaceous nanocomposites for sorbing ionizable antibiotic sulfamethazine from aqueous solution, *Water Res.* 95 (2016) 103–112.
- [6] J. Wan, G. Zeng, D. Huang, C. Huang, C. Lai, N. Li, Z. Wei, P. Xu, X. He, M. Lai, Y. He, The oxidative stress of *Phanerochaete chrysosporium* against lead toxicity, *Appl. Biochem. Biotechnol.* 175 (2015) 1981–1991.
- [7] W.W. Tang, G.M. Zeng, J.L. Gong, J. Liang, P. Xu, C. Zhang, B.B. Huang, Impact of humic/fulvic acid on the removal of heavy metals from aqueous solutions using nanomaterials: a review, *Sci. Total Environ.* 468–469 (2014) 1014–1027.
- [8] P. Xu, G.M. Zeng, D.L. Huang, C.L. Feng, S. Hu, M.H. Zhao, C. Lai, Z. Wei, C. Huang, G.X. Xie, Z.F. Liu, Use of iron oxide nanomaterials in wastewater treatment: a review, *Sci. Total Environ.* 424 (2012) 1–10.
- [9] J.L. Gong, B. Wang, G.M. Zeng, C.P. Yang, C.G. Niu, Q.Y. Niu, W.J. Zhou, Y. Liang, Removal of cationic dyes from aqueous solution using magnetic multi-wall carbon nanotube nanocomposite as adsorbent, *J. Hazard. Mater.* 164 (2009) 1517–1522.
- [10] P.A. Xu, G.M. Zeng, D.L. Huang, C. Lai, M.H. Zhao, Z. Wei, N.J. Li, C. Huang, G.X. Xie, Adsorption of Pb(II) by iron oxide nanoparticles immobilized *Phanerochaete chrysosporium*: Equilibrium, kinetic, thermodynamic and mechanisms analysis, *Chem. Eng. J.* 203 (2012) 423–431.
- [11] D.L. Huang, G.M. Zeng, C.L. Feng, S. Hu, X.Y. Jiang, L. Tang, F.F. Su, Y. Zhang, W. Zeng, H.L. Liu, Degradation of lead-contaminated lignocellulosic waste by *Phanerochaete chrysosporium* and the reduction of lead toxicity, *Environ. Sci. Technol.* 42 (2008) 4946–4951.
- [12] L. Hu, G. Zeng, G. Chen, H. Dong, Y. Liu, J. Wan, A. Chen, Z. Guo, M. Yan, H. Wu, Treatment of landfill leachate using immobilized *Phanerochaete chrysosporium* loaded with nitrogen-doped TiO₂ nanoparticles, *J. Hazard. Mater.* 301 (2016) 106–118.
- [13] M. Chen, X.M. Li, Q. Yang, G.M. Zeng, Y. Zhang, D.X. Liao, J.J. Liu, J.M. Hu, L. Guo, Total concentrations and speciation of heavy metals in municipal sludge from Changsha, Zhuzhou and Xiangtan in middle-south region of China, *J. Hazard. Mater.* 160 (2008) 324–329.
- [14] G.M. Zeng, M. Chen, Z.T. Zeng, Risks of neonicotinoid pesticides, *Science* 340 (2013), 1403–1403.
- [15] G.M. Zeng, M. Chen, Z.T. Zeng, Shale gas: surface water also at risk, *Nature* 499 (2013), 154–154.
- [16] X. Yuan, H. Huang, G. Zeng, H. Li, J. Wang, C. Zhou, H. Zhu, X. Pei, Z. Liu, Z. Liu, Total concentrations and chemical speciation of heavy metals in liquefaction residues of sewage sludge, *Bioresour. Technol.* 102 (2011) 4104–4110.
- [17] C.M. Davidson, A.L. Duncan, D. Littlejohn, A.M. Ure, L.M. Garden, A critical evaluation of the three-stage BCR sequential extraction procedure to assess the potential mobility and toxicity of heavy metals in industrially-contaminated land, *Anal. Chim. Acta* 363 (1998) 45–55.
- [18] M. Saedi, L. Li, A. Karbassi, A. Zanjani, Sorbed metals fractionation and risk assessment of release in river sediment and particulate matter, *Environ. Monit. Assess.* 185 (2013) 1737–1754.
- [19] M.H. Paller, A.S. Knox, Amendments for the in situ remediation of contaminated sediments: evaluation of potential environmental impacts, *Sci. Total Environ.* 408 (2010) 4894–4900.
- [20] S. Mignardi, A. Corami, V. Ferrini, Evaluation of the effectiveness of phosphate treatment for the remediation of mine waste soils contaminated with Cd, Cu, Pb, and Zn, *Chemosphere* 86 (2012) 354–360.
- [21] A.S. Knox, D.I. Kaplan, M.H. Paller, Phosphate sources and their suitability for remediation of contaminated soils, *Sci. Total Environ.* 357 (2006) 271–279.
- [22] P. Miretzky, A. Fernandez-Cirelli, Phosphates for Pb immobilization in soils: a review, *Environ. Chem. Lett.* 6 (2008) 121–133.
- [23] J.C. Zwönitzer, G.M. Pierzynski, G.M. Hettiarachchi, Effects of phosphorus additions on lead, cadmium, and zinc bioavailabilities in a metal-contaminated soil, *Water Air Soil Poll.* 143 (2003) 193–209.
- [24] R. Liu, D. Zhao, Synthesis and characterization of a new class of stabilized apatite nanoparticles and applying the particles to in situ Pb immobilization in a fire-range soil, *Chemosphere* 91 (2013) 594–601.
- [25] T.T. Eighty, B.S. Crannell, L.G. Butler, F.K. Cartledge, E.F. Emery, D. Oblas, J.E. Krzanowski, J.D. Eusden, E.L. Shaw, C.A. Francis, Heavy metal stabilization in municipal solid waste combustion dry scrubber residue using soluble phosphate, *Environ. Sci. Technol.* 31 (1997) 3330–3338.
- [26] R. Liu, D. Zhao, Reducing leachability and bioaccessibility of lead in soils using a new class of stabilized iron phosphate nanoparticles, *Water Res.* 41 (2007) 2491–2502.
- [27] R. Liu, D. Zhao, In situ immobilization of Cu(II) in soils using a new class of iron phosphate nanoparticles, *Chemosphere* 68 (2007) 1867–1876.
- [28] D.G. Straw, D.L. Sparks, Effects of soil organic matter on the kinetics and mechanisms of Pb(II) sorption and desorption in soil, *Soil Sci. Soc. Am. J.* 64 (2000) 144–156.
- [29] H.J. Xu, X.H. Wang, H. Li, H.Y. Yao, J.Q. Su, Y.G. Zhu, Biochar impacts soil microbial community composition and nitrogen cycling in an acidic soil planted with rape, *Environ. Sci. Technol.* 48 (2014) 9391–9399.
- [30] M.C. García, J.A. Díez, A. Vallejo, L. García, M.C. Cartagena, Effect of applying soluble and coated phosphate fertilizers on phosphate availability in calcareous soils and on P absorption by a rye-grass crop, *J. Agric. Food. Chem.* 45 (1997) 1931–1936.
- [31] G. Rauret, J.F. Lopez-Sánchez, A. Sahuquillo, R. Rubio, C. Davidson, A. Ure, P. Quevauviller, Improvement of the BCR three step sequential extraction procedure prior to the certification of new sediment and soil reference materials, *J. Environ. Monit.* 1 (1999) 57–61.
- [32] X. Gao, C.T.A. Chen, G. Wang, Q. Xue, C. Tang, S. Chen, Environmental status of Daya Bay surface sediments inferred from a sequential extraction technique, *Estuar. Coast. Shelf Sci.* 86 (2010) 369–378.
- [33] H. Akcay, A. Oguz, C. Karapire, Study of heavy metal pollution and speciation in Buyak Menderes and Gediz river sediments, *Water Res.* 37 (2003) 813–822.
- [34] A. Xenidis, C. Stouraiti, N. Papassiopi, Stabilization of Pb and As in soils by applying combined treatment with phosphates and ferrous iron, *J. Hazard. Mater.* 177 (2010) 929–937.
- [35] R.H. BRAY, L.T. KURTZ, Determination of total, organic, and available forms of phosphorus in soils, *Soil Sci.* 59 (1945) 39–46.
- [36] A. Mehlich, Mehlich 3 soil test extractant: a modification of Mehlich 2 extractant, *Commun. Soil Sci. Plan.* 15 (1984) 1409–1416.
- [37] D.W. Nelson, L.E. Sommers, A. Rapid, Accurate procedure for estimation of organic carbon in soils, *Proc. Indiana Acad. Sci.* 84 (1975) 456–462.
- [38] I.R. Quevedo, N. Tufenkji, Mobility of functionalized quantum dots and a model polystyrene nanoparticle in saturated quartz sand and loamy sand, *Environ. Sci. Technol.* 46 (2012) 4449–4457.
- [39] F. He, D. Zhao, Response to comment on manipulating the size and dispersibility of zerovalent iron nanoparticles by use of carboxymethyl cellulose stabilizers, *Environ. Sci. Technol.* 42 (2008) 3480–3480.
- [40] Y. Zuo, G. Chen, G. Zeng, Z. Li, M. Yan, A. Chen, Z. Guo, Z. Huang, Q. Tan, Transport fate, and stimulating impact of silver nanoparticles on the removal of Cd(II) by *Phanerochaete chrysosporium* in aqueous solutions, *J. Hazard. Mater.* 285 (2013) 236–244.
- [41] F.H. Wang, F. Zhang, Y.J. Chen, J. Gao, B. Zhao, A comparative study on the heavy metal solidification/stabilization performance of four chemical solidifying agents in municipal solid waste incineration fly ash, *J. Hazard. Mater.* 300 (2015) 451–458.
- [42] A. Fuentes, M. Lloréns, J. Sáez, M.I. Aguilar, J.F. Ortuño, V.F. Meseguer, Comparative study of six different sludges by sequential speciation of heavy metals, *Bioresour. Technol.* 99 (2008) 517–525.
- [43] M.R. Wiesner, G.V. Lowry, P. Alvarez, D. Dionysiou, P. Biswas, Assessing the risks of manufactured nanomaterials, *Environ. Sci. Technol.* 40 (2006) 4336–4345.
- [44] J.G. Jiang, J. Wang, X. Xu, W. Wang, Z. Deng, Y. Zhang, Heavy metal stabilization in municipal solid waste incineration flyash using heavy metal chelating agents, *J. Hazard. Mater.* 113 (2004) 141–146.
- [45] V. Laperche, S.J. Traina, P. Gaddam, T.J. Logan, Chemical and mineralogical characterizations of Pb in a contaminated soil: reactions with synthetic apatite, *Environ. Sci. Technol.* 30 (1996) 3321–3326.
- [46] S.K. Lower, P.A. Maurice, S.J. Traina, Simultaneous dissolution of hydroxylapatite and precipitation of hydroxyapatite: direct evidence of homogeneous nucleation, *Geochim. Cosmochim. Ac.* 62 (1998) 1773–1780.
- [47] S.J. Traina, V. Laperche, Contaminant bioavailability in soils sediments, and aquatic environments, *Proc. Natl. Acad. Sci.* 96 (1999) 3365–3371.
- [48] J.A. Ryan, P. Zhang, D. Hesterberg, J. Chou, D.E. Sayers, Formation of chloropyromorphite in a lead-contaminated soil amended with hydroxyapatite, *Environ. Sci. Technol.* 35 (2001) 3798–3803.
- [49] M. Chen, S.H. Daroub, L.Q. Ma, W.G. Harris, X. Cao, Characterization of lead in soils of a rifle/pistol shooting range in central Florida, USA, *Soil Sediment Contam.* 11 (2002) 1–17.
- [50] J. Yang, D.E. Mosby, S.W. Casteel, R.W. Blanchard, Lead immobilization using phosphoric acid in a smelter-contaminated urban soil, *Environ. Sci. Technol.* 35 (2001) 3553–3559.

- [51] H.M. Selim, Phosphate in Soils: Interaction with Micronutrients, Radionuclides and Heavy Metals, CRC Press, 2015.
- [52] T. Suzuki, K. Ishigaki, M. Miyake, Synthetic hydroxyapatites as inorganic cation exchangers. Part 3.—Exchange characteristics of lead ions (Pb^{2+}), J. Chem. Soc. Faraday Trans. 1: Phys. Chem. Condens. Phases 80 (1984) 3157–3165.
- [53] W.L. Lindsay, Chemical Equilibria in Soils, John Wiley and Sons Ltd., 1979.
- [54] Y. Takeuchi, T. Suzuki, H. Arai, A study of equilibrium and mass transfer in processes for removal of heavy-metal ions by hydroxyapatite, J. Chem. Eng. Jpn. 21 (1988) 98–100.
- [55] U. Thawornchaisit, C. Polprasert, Evaluation of phosphate fertilizers for the stabilization of cadmium in highly contaminated soils, J. Hazard. Mater. 165 (2009) 1109–1113.
- [56] M. Chrysochoou, D. Dermatas, D.G. Grubb, Phosphate application to firing range soils for Pb immobilization: the unclear role of phosphate, J. Hazard. Mater. 144 (2007) 1–14.
- [57] R. Liu, D. Zhao, Reducing leachability and bioaccessibility of lead in soils using a new class of stabilized iron phosphate nanoparticles, Water Res. 41 (2007) 2491–2502.
- [58] D.F. Malley, P.C. Williams, Use of near-infrared reflectance spectroscopy in prediction of heavy metals in freshwater sediment by their association with organic matter, Environ. Sci. Technol. 31 (1997) 3461–3467.
- [59] T. Ohno, T.B. Parr, M.C.I. Gruselle, I.J. Fernandez, R.L. Sleigher, P.G. Hatcher, Molecular composition and biodegradability of soil organic matter: a case study comparing two New England forest types, Environ. Sci. Technol. 48 (2014) 7229–7236.
- [60] M. Šmejkalová, O. Mikánová, L. Borůvka, Effects of heavy metal concentrations on biological activity of soil micro-organisms, Plant Soil Environ. 49 (2003) 321–326.
- [61] A. Austruy, M. Shahid, T. Xiong, M. Castrec, V. Payre, N.K. Niazi, M. Sabir, C. Dumat, Mechanisms of metal-phosphates formation in the rhizosphere soils of pea and tomato: environmental and sanitary consequences, J. Soil. Sediment. 14 (2014) 666–678.
- [62] J.G. Lin, S.Y. Chen, The relationship between adsorption of heavy metal and organic matter in river sediments, Environ. Int. 24 (1998) 345–352.